Steady state and dynamic operation of four-product dividing-wall (Kaibel) columns: Experimental Verification

Journal:	*Industrial & Engineering Chemistry Research*
Manuscript ID:	ie-2012-01432z
Manuscript Type:	Article
Date Submitted by the Author:	31-May-2012

Complete List of Authors:	Dwivedi, Deeptanshu; Norwegian University of Science and Technology, Trondheim, Norway, Chemical Engineering Strandberg, Jens; Aker Solutions, Halvorsen, Ivar; SINTEF, Applied Cybernetics Skogestad, Sigurd; Norwegian University of Science and Technology, Chemical Engineering Department

Steady state and dynamic operation of four-product dividing-wall (Kaibel) columns: Experimental Verification

Deeptanshu Dwivedi,[†] Jens P. Strandberg,[†,¶] Ivar J. Halvorsen,[‡] and Sigurd Skogestad[*,†]

Department of Chemical Engineering, Norwegian University of Science and Technology, Trondheim, and Applied Cybernetics, SINTEF, Trondheim

E-mail: skoge@ntnu.no

Abstract

Control and operation of energy-efficient arrangements, including dividing-wall columns, can be challenging. This paper demonstrates experimentally the start-up and steady state operation of a four product Kaibel column separating methanol, ethanol, propanol and *n*-butanol. We use a control structure with four temperature controllers and show that it can handle feed rate disturbances as well as setpoint changes. The experimental data compares well with an equilibrium stage model and such models can be used for design and predicting optimal operation.

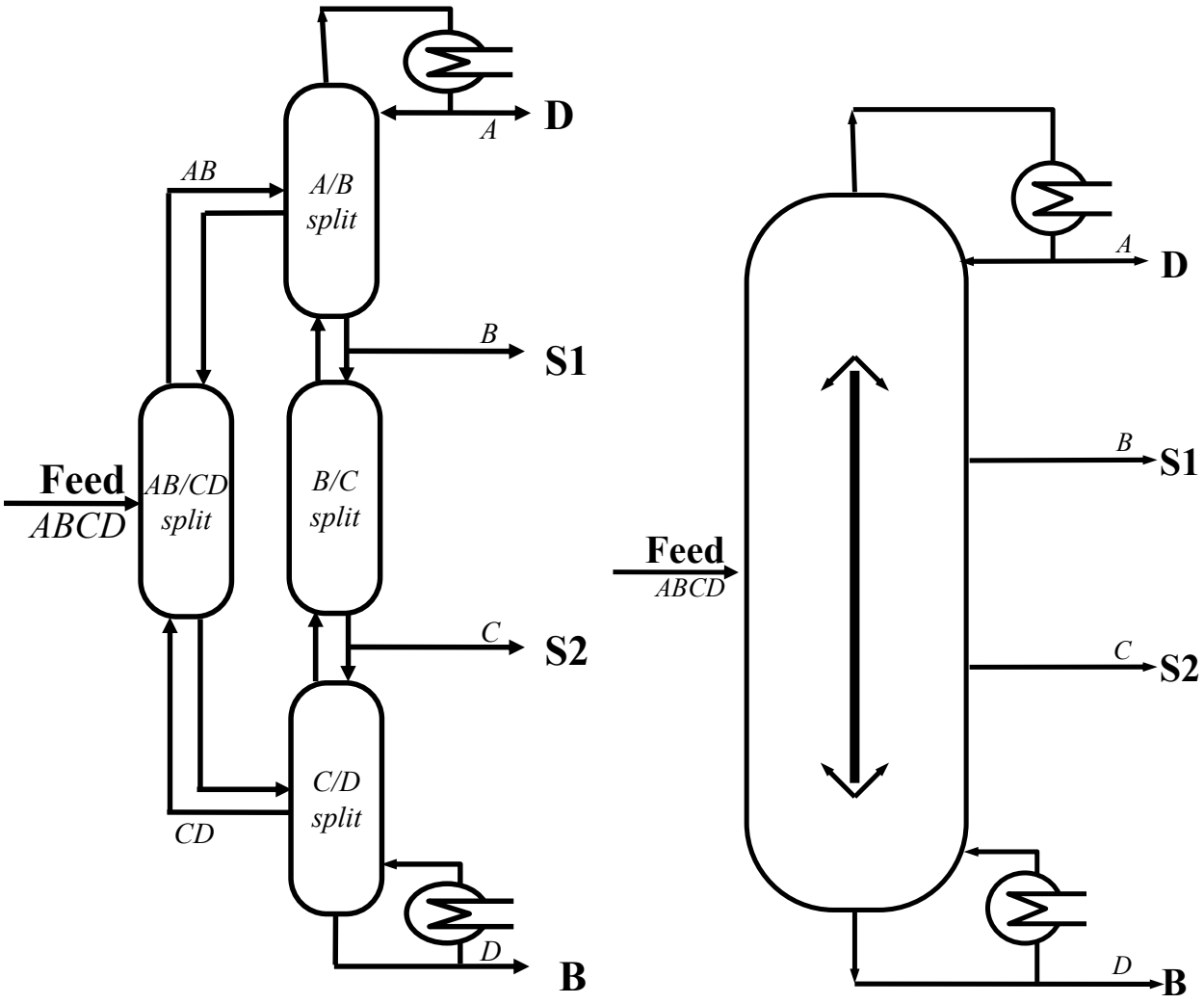

(a) *Implementation with four separate column sections*[1] (b) *Dividing-wall implementation with two side products*[2]

Figure 1: Thermodynamically equivalent implementations of four-product Kaibel column (studied in this paper)

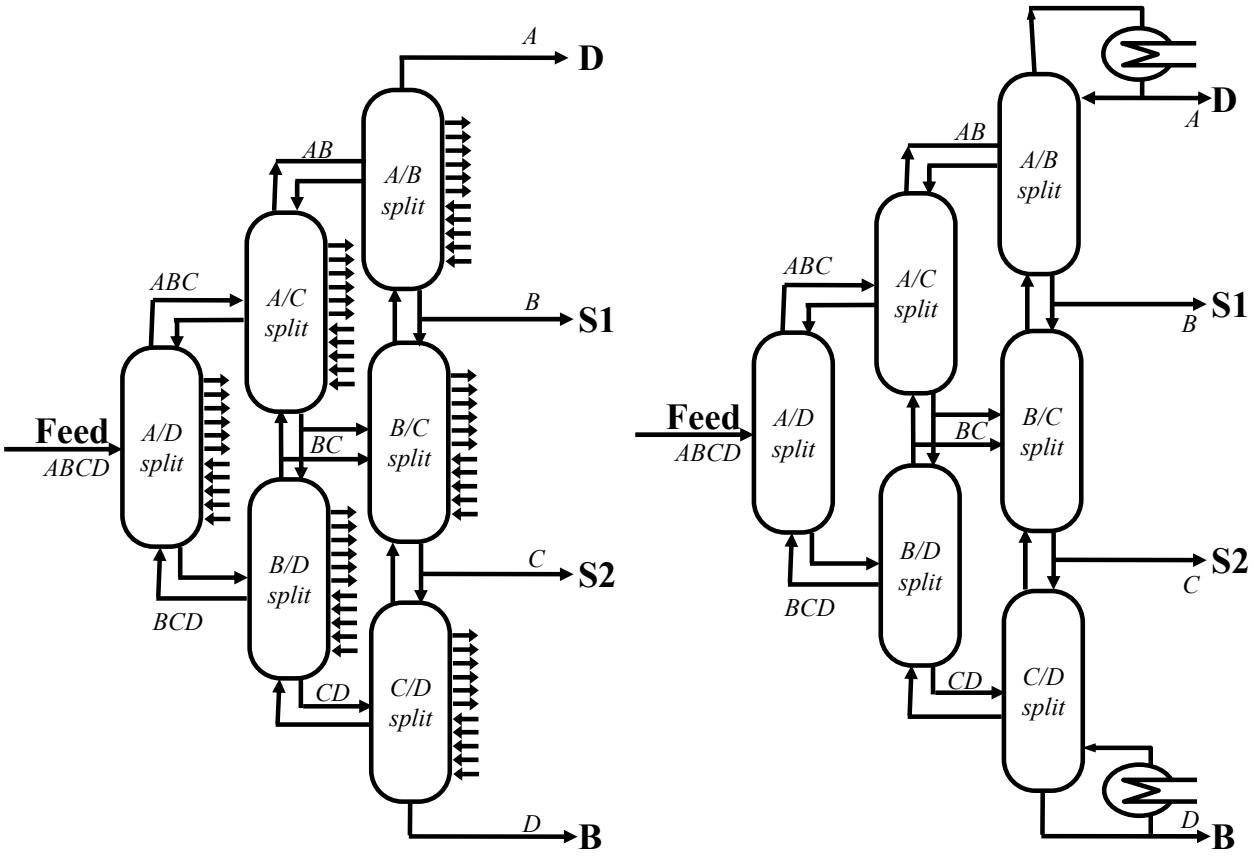

(a) *Four-product "reversible" Petlyuk column* (b) *Four-product adiabatic Petlyuk column*

Figure 2: "Reversible" and adiabatic arrangements of Four-product "extended" Petlyuk column (*not* studied in this paper)

Introduction

Distillation is a separation technique that uses heat energy to provide the separation work of "unmixing" the feed mixture. In this paper we study the integrated Kaibel distillation scheme for separation of four components as shown in Figure 1.[2] The main motivation for this scheme is combination of capital savings and energy savings compared to conventional distillation sequences for multicomponent separation. This scheme is not the best in terms of minimum separation work (exergy), mainly because it performs a difficult B/C split in the prefractionator and not the easiest (A/D) split.

An "ideal reversible" system with minimum exergy requires a more complex arrangement, infinite number of stages and heating and cooling on all stages.[3–5] For four-product separation, Figure 2a shows the reversible scheme proposed by Petlyuk and Platonov.[6] The column sections are directly coupled and the easiest split is done first. Any mixing losses near the feed stage and at the ends can thus be avoided.

Some of the features of reversible distillation are retained in an adiabatic "four-product extended Petlyuk column", which has only one heater (reboiler) and one cooler (condenser) (See Figure 2b). In fact, the adiabatic scheme shown in Figure 2b is better than the reversible scheme in Figure 2a in terms of energy although it is inferior in terms of exergy. Compared to conventional two-product column sequences, the potential energy savings in an adiabatic "four-product extended Petlyuk arrangement" (Figure 2b) can be up to 50%.

The disadvantage of using the arrangements shown in Figure 2 is that, a large number of sections are required for a multicomponent separation. Petlyuk et al.[1] also proposed schemes for multicomponent separation with a minimum number of column sections. Thermodynamically, this is equivalent to the scheme proposed later by Kaibel[2] with a vertical partition or dividing-wall (see Figure 1b). For a four-product separation, the scheme given by Petlyuk is same as the

*To whom correspondence should be addressed
†Department of Chemical Engineering, Norwegian University of Science and Technology
‡Applied Cybernetics, SINTEF, Trondheim
¶Presently: Senior Process Engineer, Aker Solutions, Norway

"Kaibel" scheme in figure 1a.[7] The four product Kaibel column, in Figure 1, although less efficient than the Petlyuk arrangements in Figure 2 can still offer up to 30% energy saving compared to conventional sequences due to the directly coupled prefractionator.[8] Our experimental setup is similar to the scheme in Figure 1a, which does not have a vertical dividing-wall but the results are extendable to dividing-wall columns.

Numerous successful industrial implementation of three-product dividing-wall columns have been reported by the German company BASF,[9,10] but less is reported on control and operation of such columns. In the open literature, a thorough experimental study for operation of a three-product high purity distillation column was reported Niggemann et al..[11] Earlier, start-up for a three-product column based on rigorous simulations was reported by Niggemann et al..[12] Mutalib and Smith[13] reported a simulation study on three-product dividing column and concluded that a conventional proportional-integral (PI) control scheme can give good regulation. They also reported experimental studies done on a pilot plant column.[14] Adrian et al.[15] reported that a multivariable model predictive control can give tighter control and shorter time to steady state in an experimental dividing-wall column. Ling and Luyben[16] performed a simulation study and proposed a four-point control structure for a three-product dividing-wall column.

There is one reported use of four-product Kaibel column in BASF and several patents from BASF as summarized by Dej.[10] Some simulation work has also been carried out on control and operation of four-product Kaibel column. Strandberg and Skogestad[17] found in a simulation study that a four-point temperature control scheme with one temperature controlled in the prefractionator together with the inventory control can stabilize the column and prevent 'drift' of the composition profiles during operation. Ghadrdan et al.[18] reported another simulation study on optimal steady state operating solutions for economic criterions like minimizing energy for fixed purity specifications. Kvernland et al.[19] studied a multivariable Model Predictive Controller on top of a regulatory layer with a four-point temperature control.

However, in the open literature, there are no experimental studies reported on operation and control of four-product directly coupled columns. In this paper we present experimental results

for a four-product Kaibel column separating methanol, ethanol, 1-propanol and 1-butanol (with normal boiling points of 64.7 ^{0}C, 78.4 ^{0}C, 97.2 ^{0}C and 117.7 ^{0}C, respectively).

Experimental setup

Figure 3a shows a picture of our experimental column.[20] Although this is not a dividing-wall column, it is thermodynamically equivalent as illustrated in Figure 1. The height of the column is about 8 meters. The system is operated at atmospheric pressure and the column sections are packed with 6-mm glass Raschig rings. The reboiler is kettle type and the power to the reboiler is adjusted by varying the voltage to the heater elements through a thyristor. The condenser is mounted on top of the column and is water-cooled. The condensed vapor flows back to the column due to gravity; a part is take out as top product and the rest forms the liquid reflux. The control setup is implemented in Lab View^{TM} on a standard PC.

The liquid reflux split valve, top product valve and side product valve are swinging funnels (On/ Off) and are controlled by externally placed solenoids. The flow through the swinging funnel depends on the internal liquid flows in the respective column section. To implement the continuous output of the proportional-integrator (PI) controllers, the common technique of pulse width modulation (PWM) is used. The switching frequency of the On/ Off valves is much faster than the plant dynamics and hence emulates continuous-pump flow conditions. The valve switching function has a total cycle time of 10 seconds and the resolution time for switching is 0.2 seconds. For example, if the controller output is 0.22, a valve position on one side of the funnel is 2.2 seconds and 7.8 seconds on the other. This gives an implemented accuracy of 4% when the valve position is 0.5, but much worse resolution when close to the fully open (0)/ close (1) position. To improve the resolution, we used an algorithm that allows also the total cycle time to change between 5 seconds and 15 seconds. This implementation reduces the rounding off errors and improves the resolution of the valve.

In our setup, it is also possible to adjust the vapor split ratio (R_V) between the prefractionator

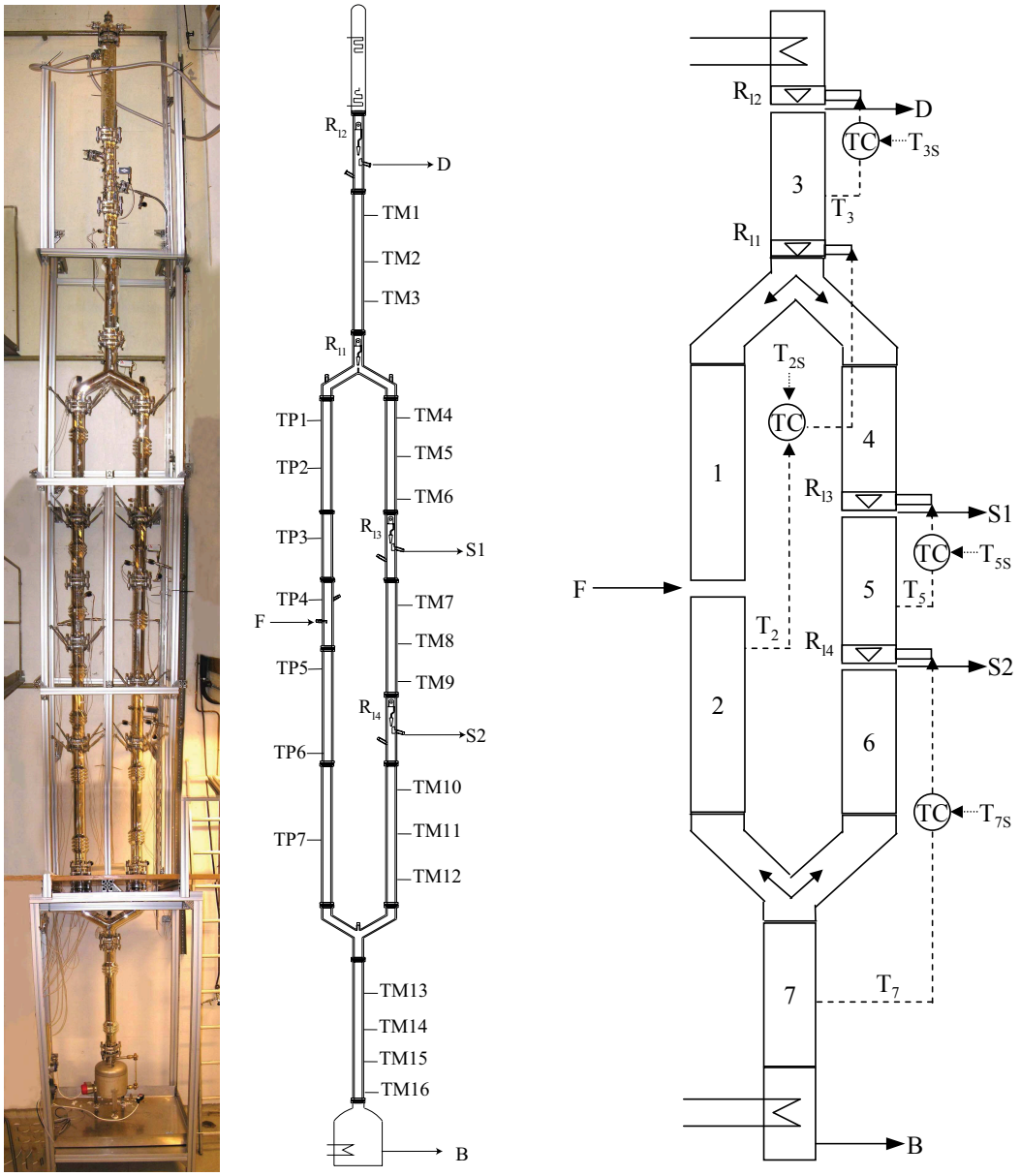

(a) (b) (c)

Figure 3: (a) Picture of the experimental column.[20]
(b) Schematic showing location of temperature sensors.[20]
(c) 4-point regulatory control structure used for operation $T_2 = \text{TP5},\ T_3 = \text{TM2},\ T_5 = \text{TM8},\ T_7 = \text{TM14}$.

and the main column using a valve, but in the reported experiments it has been kept constant. The vapor split between the prefractionator and the main column is then determined by the normal pressure drop offered by the packing in the column sections.

The liquid-level measurement in the reboiler was faulty and a level controller could not be installed. Therefore, the bottom product was allowed to accumulate during the experimental runs. With a large reboiler, the composition of the bottoms will then take a long time to reach steady state, but otherwise this should have little effect on the experimental results.

Control Structure

Table 1: Four-point temperature regulatory control structure [a,b]

Control loop	Manipulated Variable [a]	Controlled Variable [b]
Loop 1	Liquid split valve (R_{L1})	temperature in section 2 (T_2)
Loop 2	Distillate split valve (R_{L2})	temperature in section 3 (T_3)
Loop 3	Upper side product split valve (R_{L3})	temperature in section 5 (T_5)
Loop 4	Lower side product split valve (R_{L4})	temperature in section 7 (T_7)

[a] manipulated variables (controller outputs) are the swinging funnel ratios R_{L1}, R_{L2}, R_{L3} and R_{L4}: $R_{L1} = \frac{L_1}{L_3}$, $R_{L2} = \frac{L_3}{L_3+D}$, $R_{L3} = \frac{L_5}{L_5+S1}$, $R_{L4} = \frac{L_6}{L_6+S2}$
Here, L_1, L_3, L_5 and L_6 are liquid flows in sections 1, 3, 5 and 6, respectively (see Figure 3)
S1 and S2 are side product flow rates
[b] controlled variables are temperature sensors as shown in figures 3b and 3c: $T_2 = TP5$, $T_3 = TM3$, $T_5 = TM8$ and $T_7 = TM14$

As reported earlier by Strandberg and Skogestad,[17] a 4-point temperature control structure can avoid "drift" of the composition profile in the various sections of a 4-product column. In Figure 3c, we show the control structure used in the experiments. The column sections are numbered from 1 to 7. Sections 1 and 2 constitute the prefractionator, while sections 3-7 form the main column. In Table 1, we show the loop pairings used in the control structure. The four temperature control loops are named loop 1, 2, 3 and 4. In the footnote to Table 1, we also define the four corresponding liquid flow ratios R_{L1}, R_{L2}, R_{L3} and R_{L4} which are set by the swinging funnels.

In control loop 1, the liquid split ratio (R_{L1}) is used to control a sensitive temperature in the prefractionator ($T_2 =$ TP5). In loop 2, the distillate split ratio (R_{L2}) controls a temperature in section 3 ($T_3 =$ TM3). In the loop 3, the upper side product split ratio (R_{L3}) controls a sensitive temperature in section 5 ($T_5 =$ TM8). Finally, in control loop 4, the lower side product split ratio (R_{L4}) is used to control a sensitive temperature in the bottom section ($T_7 =$ TM14).

The controllers are conventional proportional-integrator (PI) controllers. As the system is interactive, we used sequential tuning and loop 1 in the prefractionator was closed first. Next loops 2, 3 and 4 in the main column were closed. The tuning of the loops was done using the SIMC rules[21] with the tuning parameter, τ_C, chosen to be 1 minute for loops 1 and 2 and 2 minutes for loops 3 and 4. The temperature setpoints for the loops were adjusted during start-up as explained below.

The remaining two degrees of freedom, the boilup (V) and the vapor split ratio (R_V), are not used for control in experiments, but may be in general be available for some optimizing objective, like minimizing energy for a given specification.

Experiments

Various experiments were conducted for studying the start-up operation, to test the 4-point control structure for setpoint changes, and disturbances and to study steady state operation. Table 2 shows a list of the 13 experiments reported in this paper.

Start-up

Figure 4 shows the results from a typical cold start-up of the pilot plant (Experimental run 1). The following start-up policy was used:

After turning on the reboiler (at time = 0), the column is heated up in total reflux mode (D=0, S1=0, S2=0, F=0). The output of control loop 1 (R_{L1}) is fixed at 0.3 (manual mode). This implies that 30% of the reflux is directed to the prefractionator using the liquid split valve. At about 30

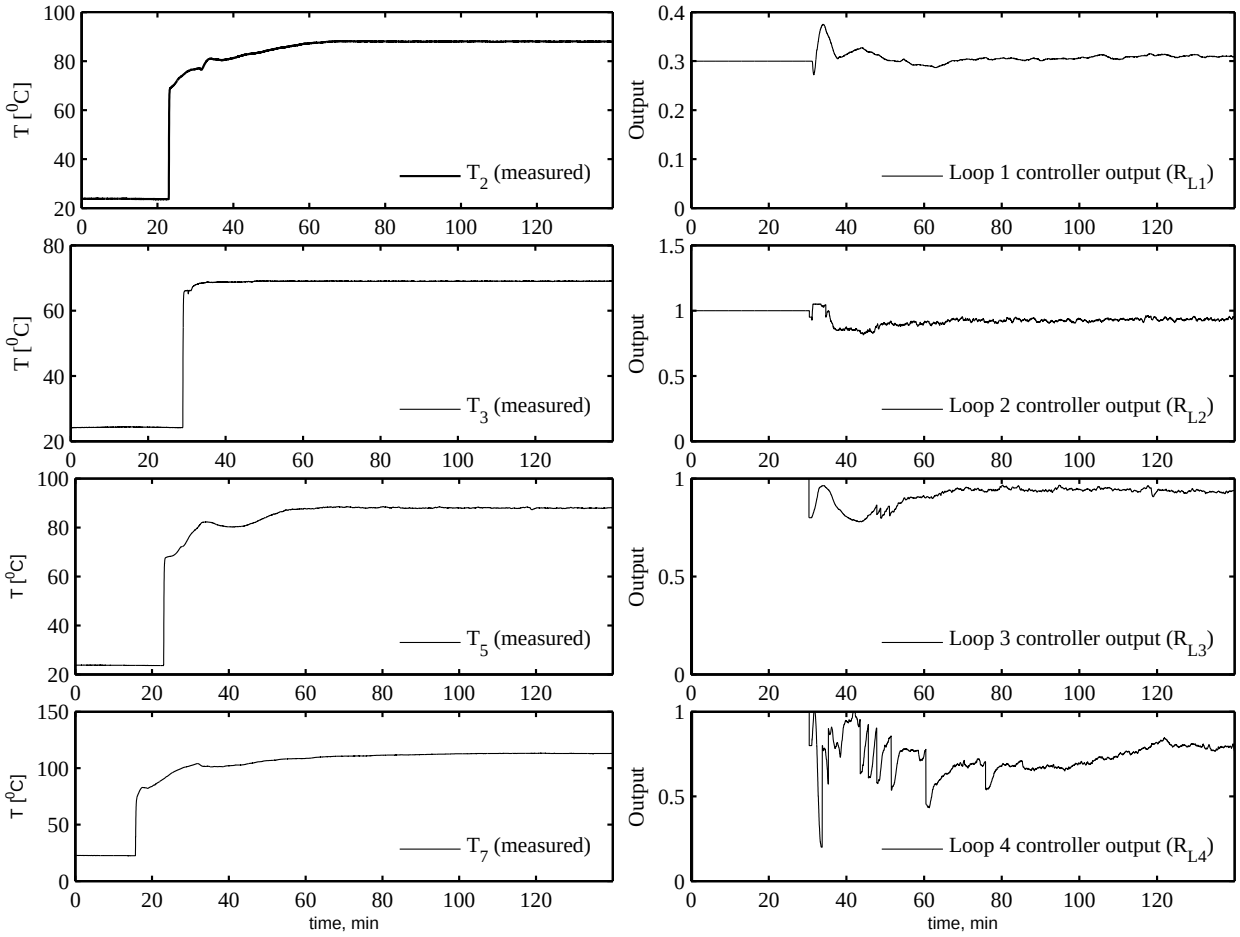

Figure 4: Experimental Run 1: Cold Start-up

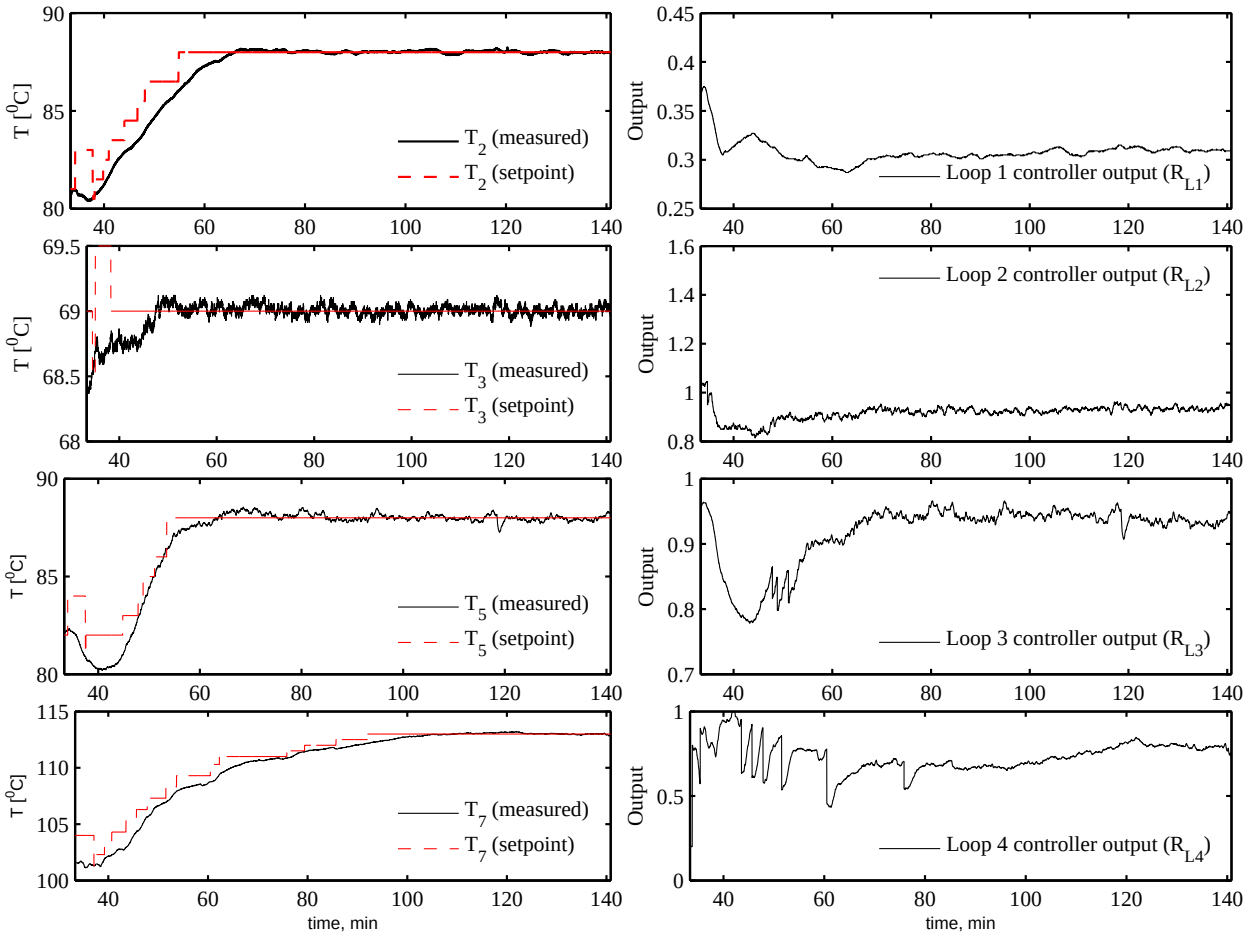

Figure 5: Experimental Run 1: Cold Start-up (Zoomed in from 35 min to 140 min)

minutes, the feed to the column is turned on. Shortly after, the controllers (loop 1, 2, 3 and 4) are turned on (AUTO mode). With control loops 2, 3 and 4 turned on, we begin to draw the three products D, S1 and S2. The initial temperature setpoints are the values from the total reflux mode, and the setpoints are then adjusted in closed-loop mode to get good separation in the column. The temperature setpoint for the prefractionator (T_{2s}) is adjusted to get a large temperature change across the prefractionator column. This corresponds to a sharp split between the intermediate components (ethanol and propanol). The setpoints for the remaining loops (T_{3s}, T_{5s} and T_{7s}) are for the main column which performs binary splits, and these are adjusted in an attempt to get the temperatures of the four product close to the normal boiling point of their corresponding main components. Off-line analysis of the products (reported later) shows that this start-up procedure resulted in good quality products, in spite of the fact that we used only temperature loops. Of course, if online composition measurements are available, these should be used to adjust the temperature setpoints.

Figure 5 shows a zoomed-in plot of Figure 4 for the time period from 35 min to 140 min. In the experiments, the feed flow rate was held constant at 3 liters/hour and the reboiler duty was set constant at 2 kW. We conclude from the experiment (Figures 4 and 5) that the start-up procedure works well and leads to stable operation.

Closed-loop operation

In the following experiments (runs 2-7), the four temperatures setpoints are changed in closed-loop, to drive the system to various new steady states. The composition of the feed mixtures is also varied.

In Figure 6 (run 2), we show results for a temperature setpoint change of $-2\ ^0$C to control loop 1. This setpoint change can be handled well and the steady state is reached in about 25 minutes. There is an initial delay of about 1 minute as the location of the temperature is far from the valve. As a consequence, it takes a while for the change in the liquid reflux to affect the controlled temperature. This loop has significant interaction with loops 3 and 4.

Figure 7 (run 3) shows a setpoint change of $\pm 1\ ^0$C change in the loop 2. Again, this setpoint

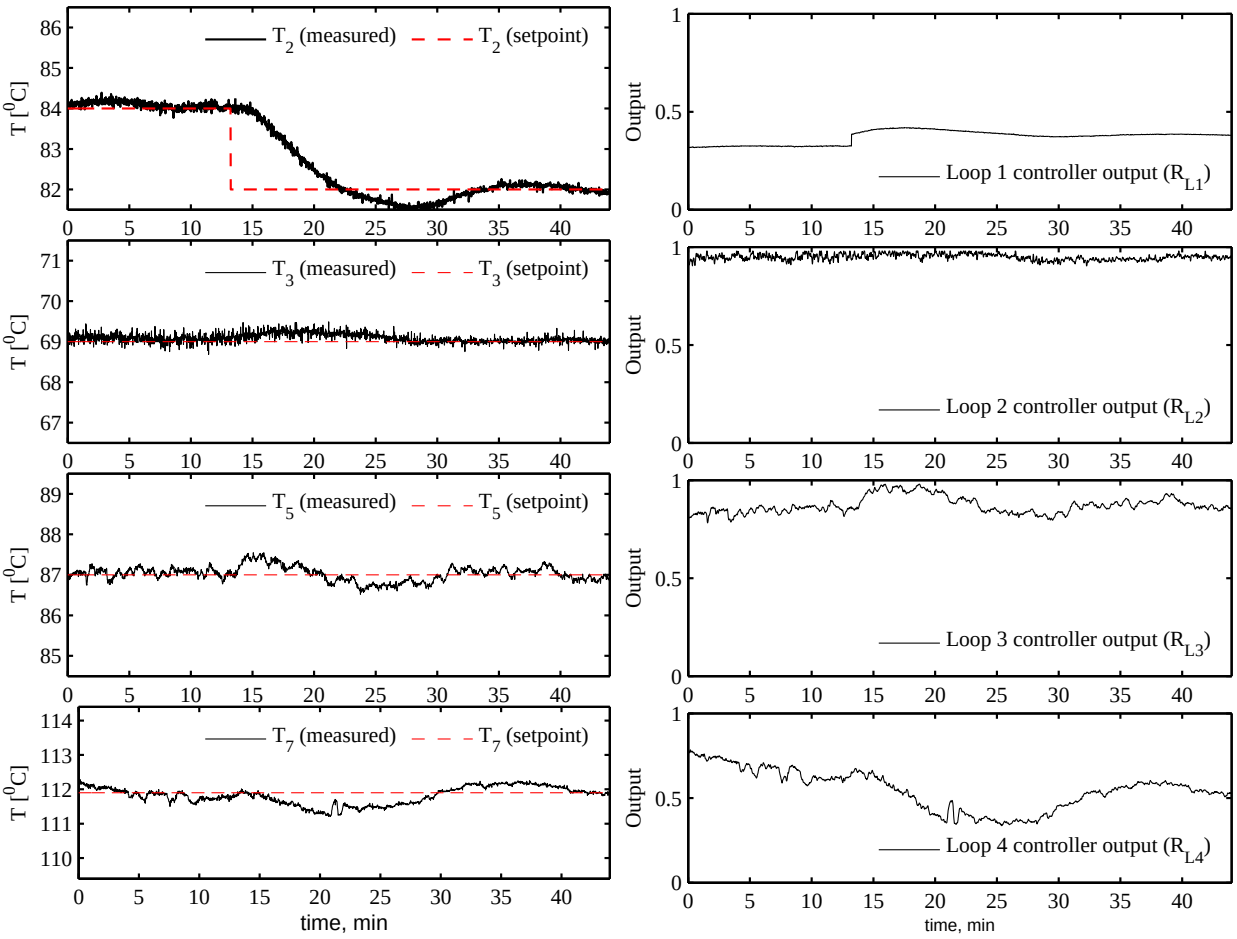

Figure 6: Experimental Run 2: $-2[^0C]$ setpoint change in prefractionator temperature, T_2 (control loop 1)

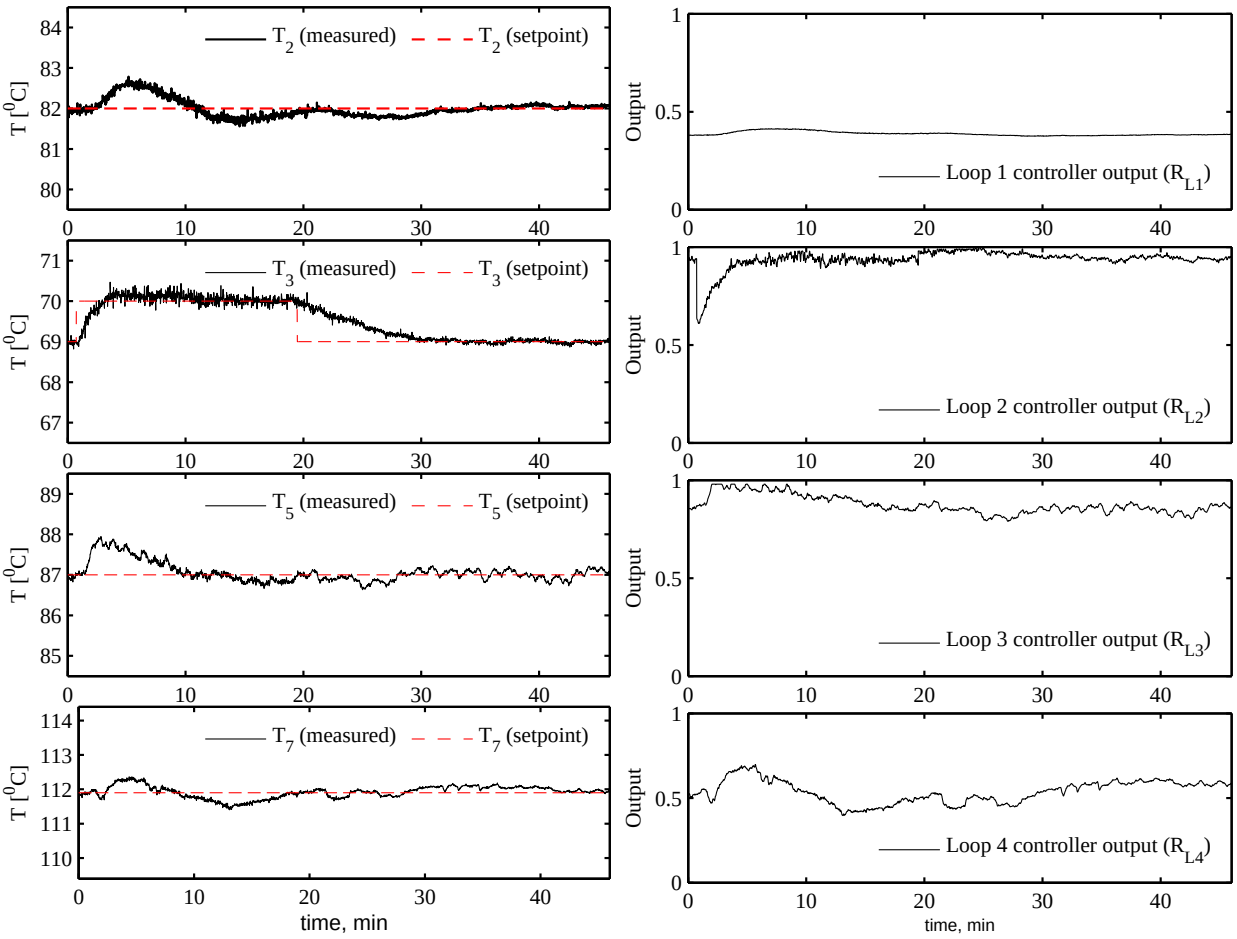

Figure 7: Experimental Run 3: $\pm$ 1 $[^0C]$ setpoint change in top section temperature, T_3 (control loop 2)

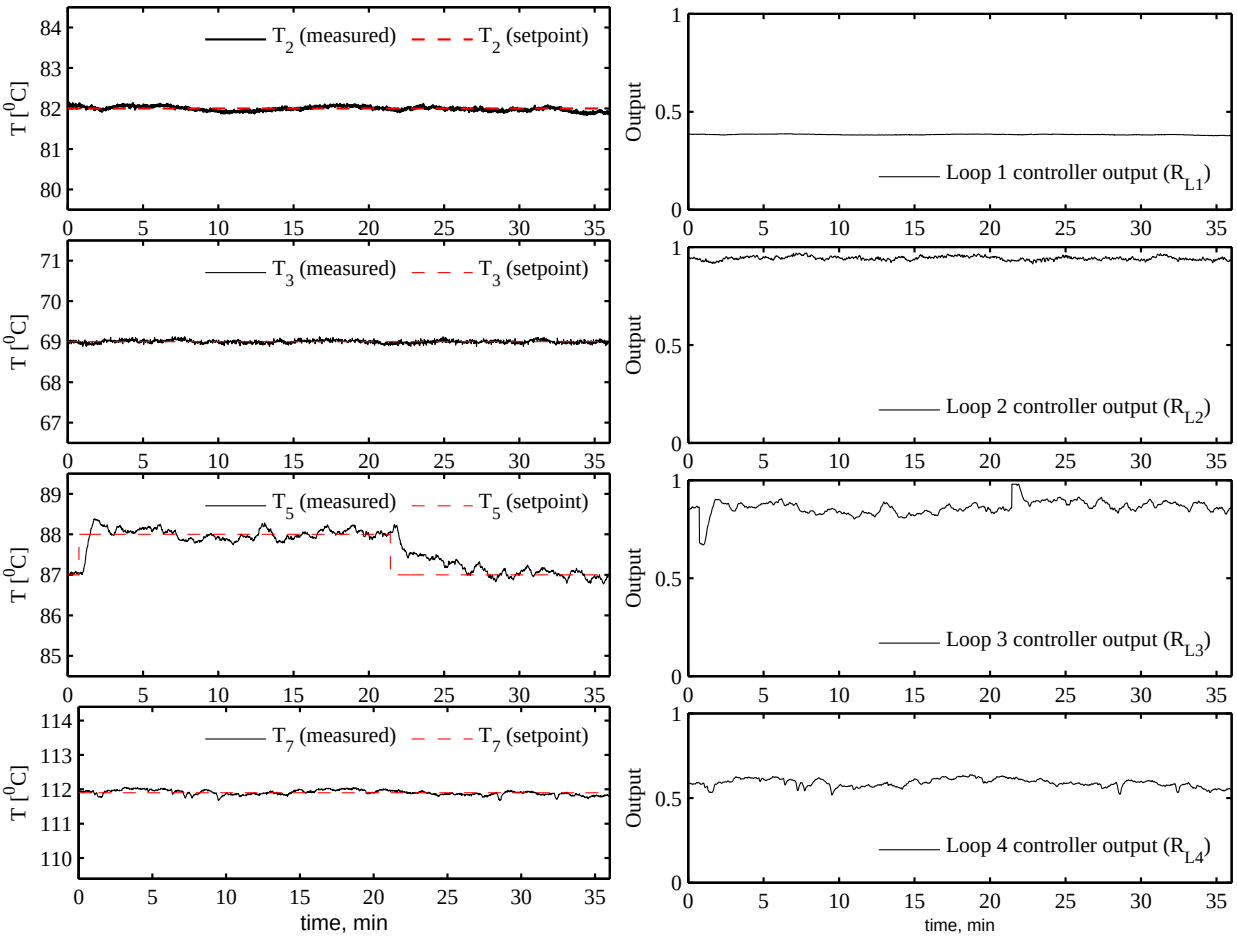

Figure 8: Experimental Run 4: $\pm$ 1 $[^0C]$ setpoint change in middle section temperature, T_5 (control loop 3)

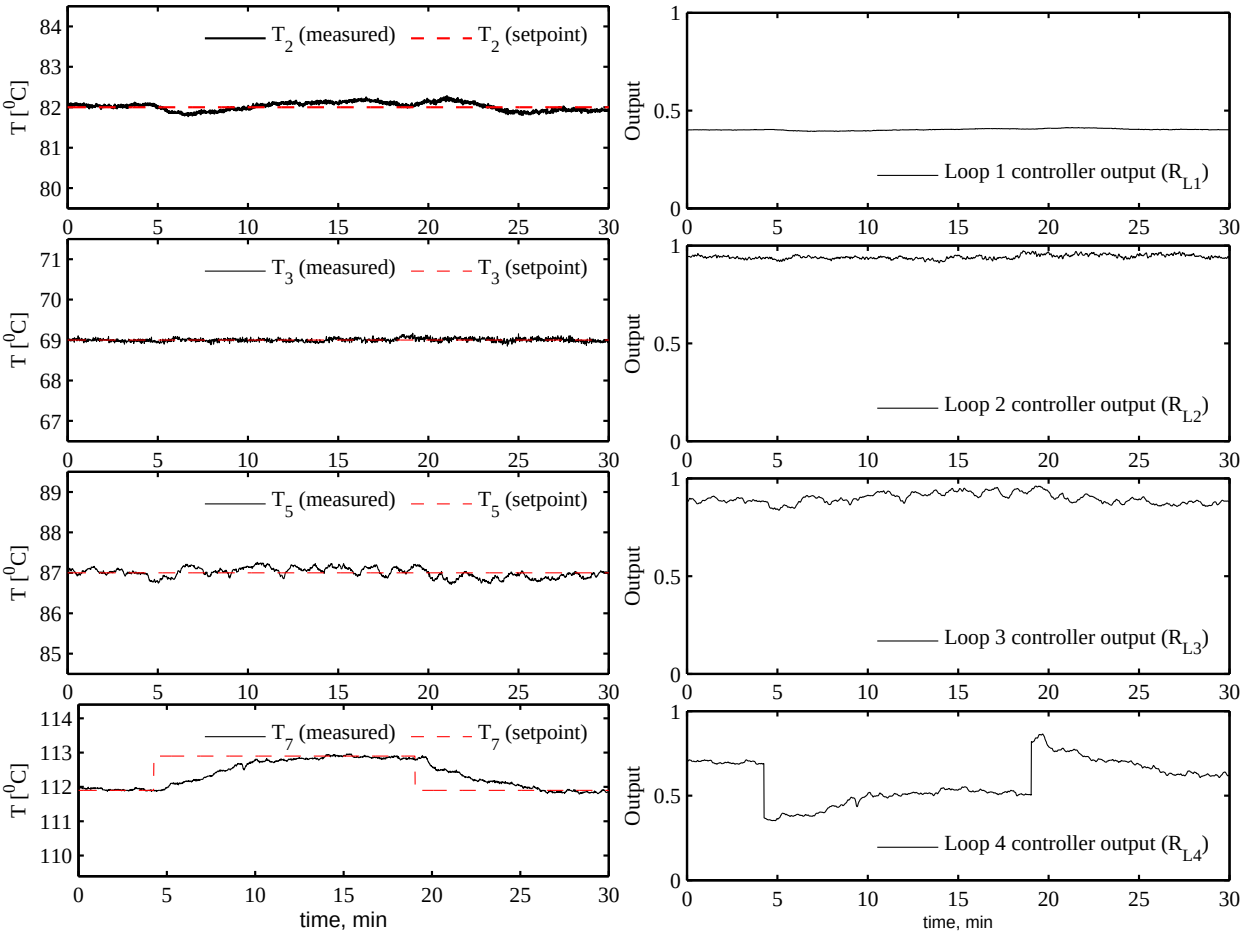

Figure 9: Experimental Run 5: $\pm$ 1 $[^0C]$ setpoint change in bottom section temperature T_7 (control loop 4)

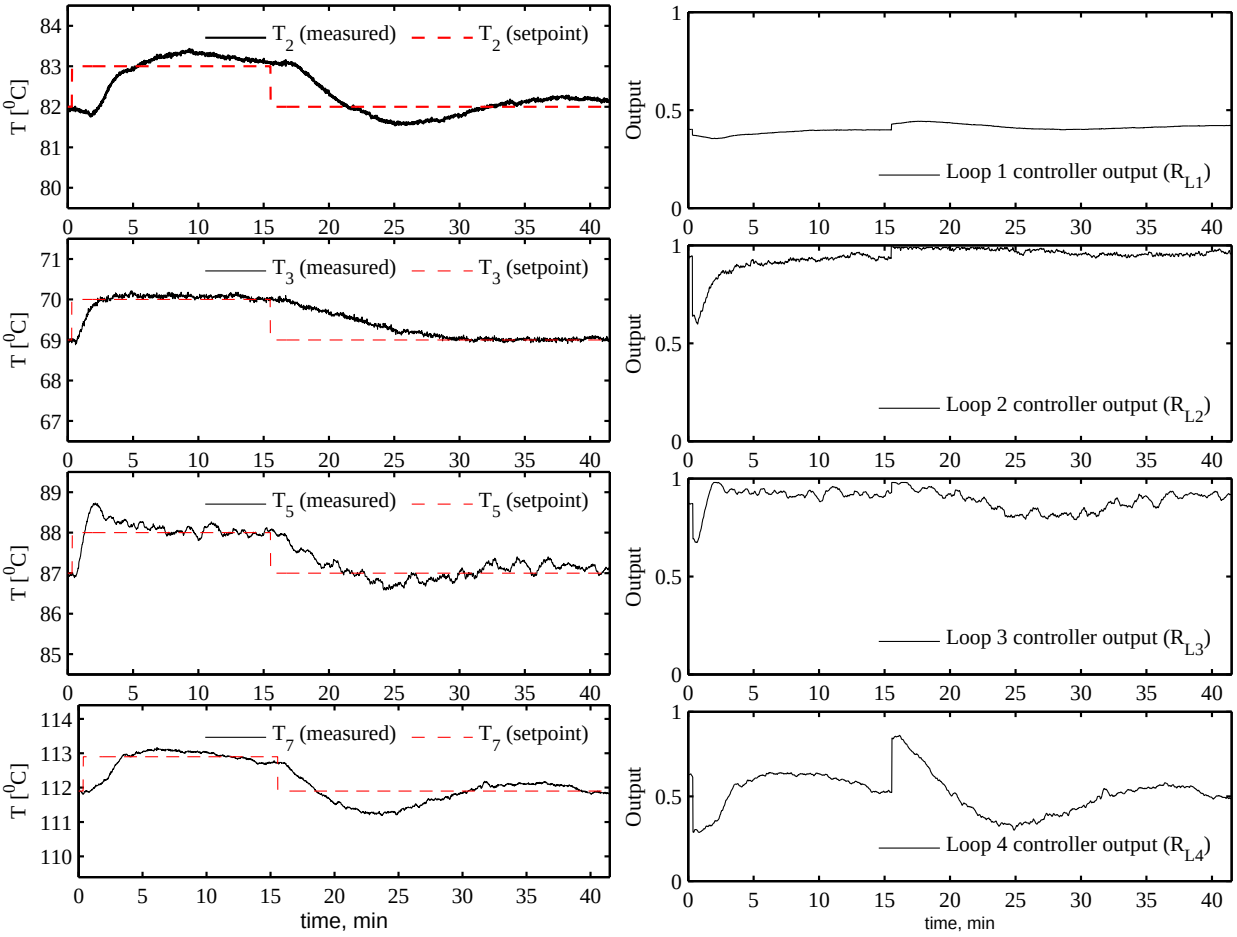

Figure 10: Experimental Run 6: Simultaneous change in all four temperature setpoints

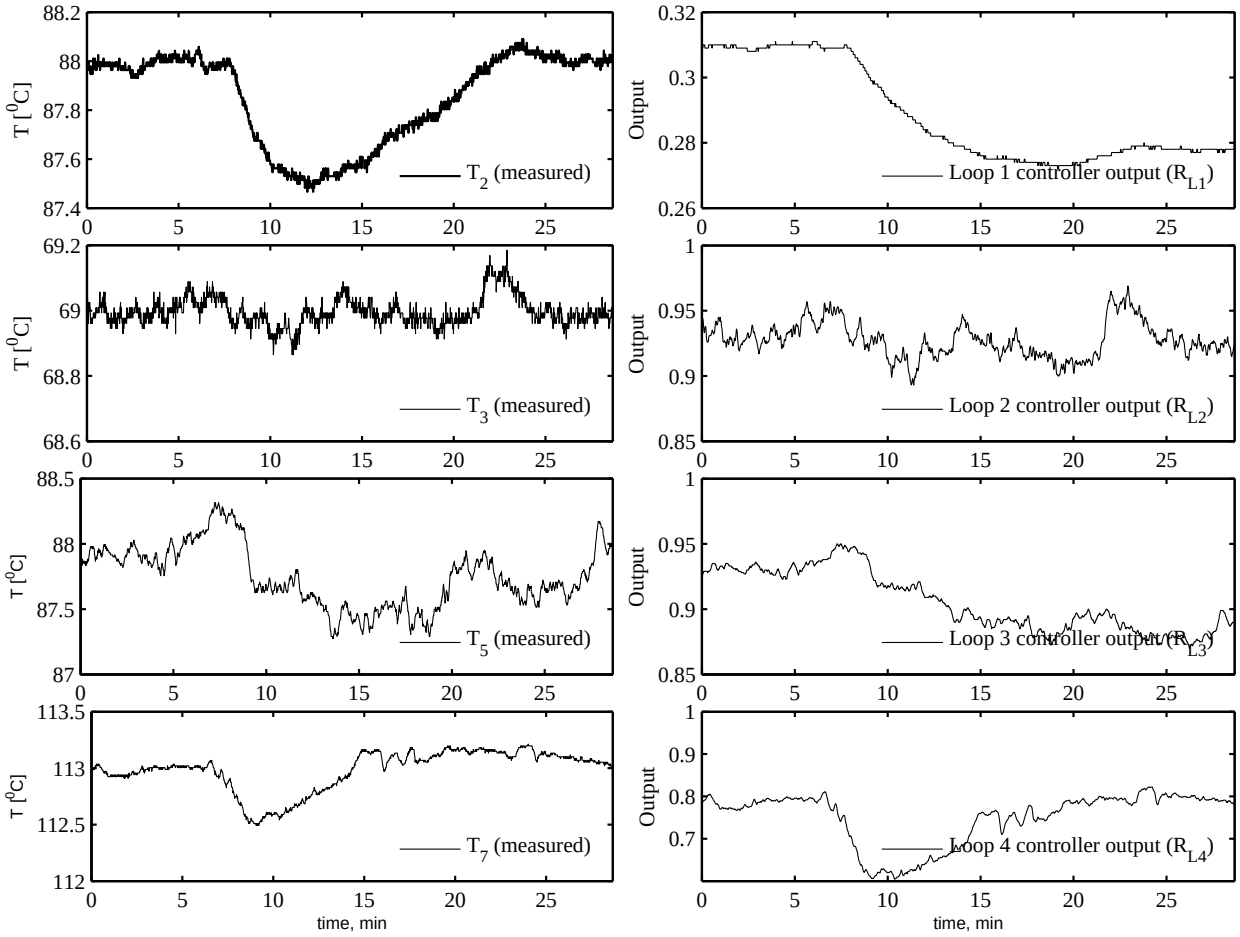

Figure 11: Experimental Run 7: +20 % feed rate disturbance (at t= 5 *min*)

change is handled well. However, there is significant interaction with all the other loops. This is because a change in distillate flow affects directly the molar difference between the boilup (V) and liquid reflux (L) in the entire column.

Figure 8 and 9 (runs 4 and 5) plot show similar setpoint changes in the loops 3 and 4, respectively and these changes are handled well without interactions with other loops. Figure 10 (run 6) shows simultaneous changes in the setpoint for all the four loops, which is also handled reasonably well.

Finally, Figure 11 (run 7) shows the response for an increase in feed rate from 3 liters/hr to 3.6 liters/hr (+20%). This disturbance can also be handled well and the controlled-temperatures are brought back to their setpoints in about 30 minutes.

Figure 14 is a screenshot from the computer interface (Lab View) during the experimental run 12, with a snapshot of temperatures as read by the probes in various sections. The dialog labelled "Temperature graphs" shows the four controlled temperatures for 100 seconds. Note that some of the temperature measurements have large measurement biases and their values are calibrated for later analysis and one probe (T15) is faulty.

Steady state experiments and comparison with simulations

Experimental runs 8-12 were run with constant temperature setpoints to steady state and for runs 9-12. Samples of the feed and products were collected and analyzed using High-performance liquid chromatography (HPLC). Figure 12 (run 8) shows a typical response when the column is "steady" for a period of 2 hours, with all the four temperature loops closed. All the four temperatures can be maintained at their respective setpoints. Figure 13 shows experiment run 9 with another constant setpoint operation. The steady-state results for run 9-12 are summarized in Table 3 (compositions) and Table 4 (controller outputs $\equiv$ plant inputs).

We now want to compare the steady-state experimental results with a standard equilibrium stage distillation model. The vapor-liquid equilibria is modelled using the Wilson model for the

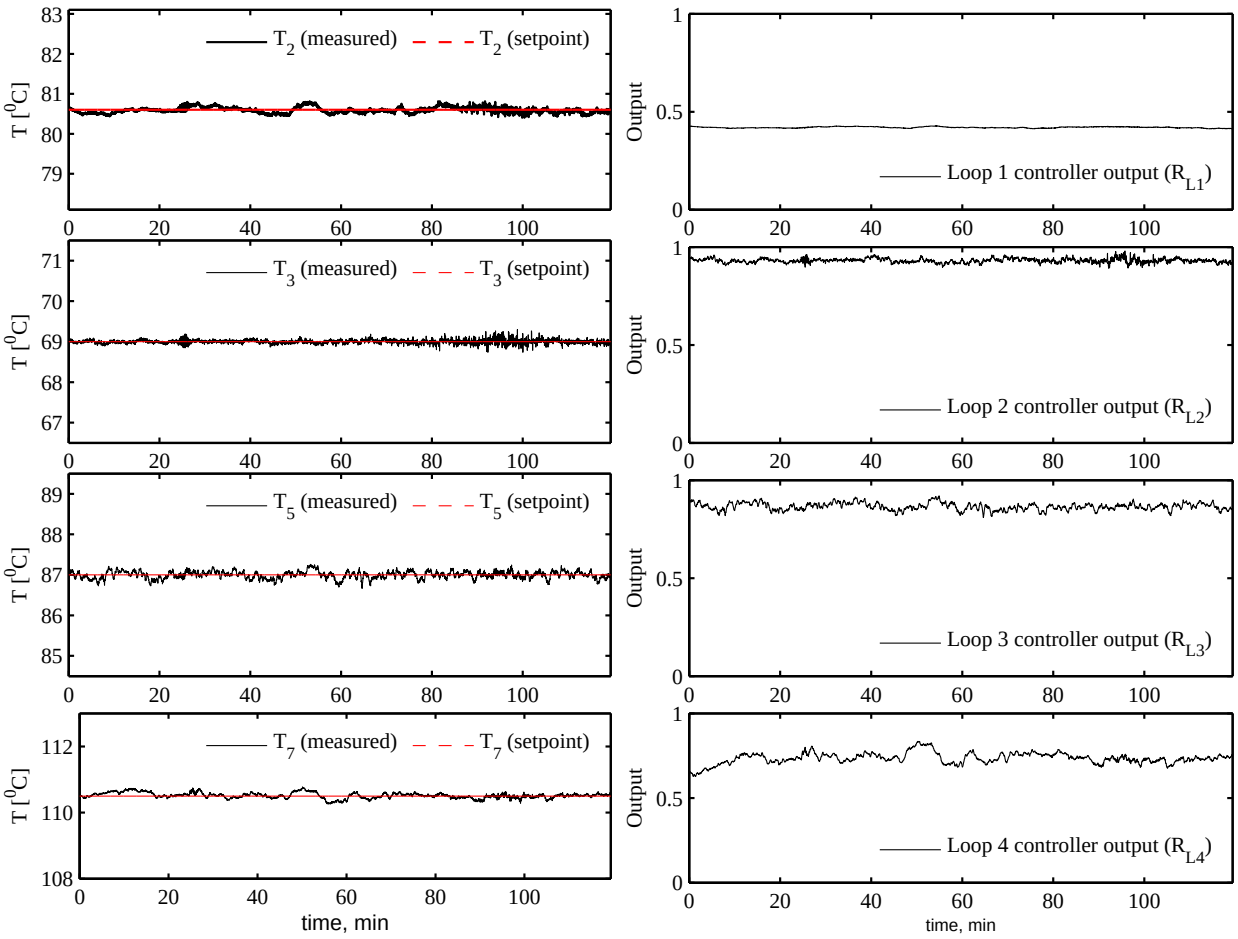

Figure 12: Experimental Run 8: steady state operation ($T_{2S} = 80.6\ ^0C\ T_{3S} = 69\ ^0C\ T_{5S} = 82\ ^0C\ T_{7S} = 110.2\ ^0C$)

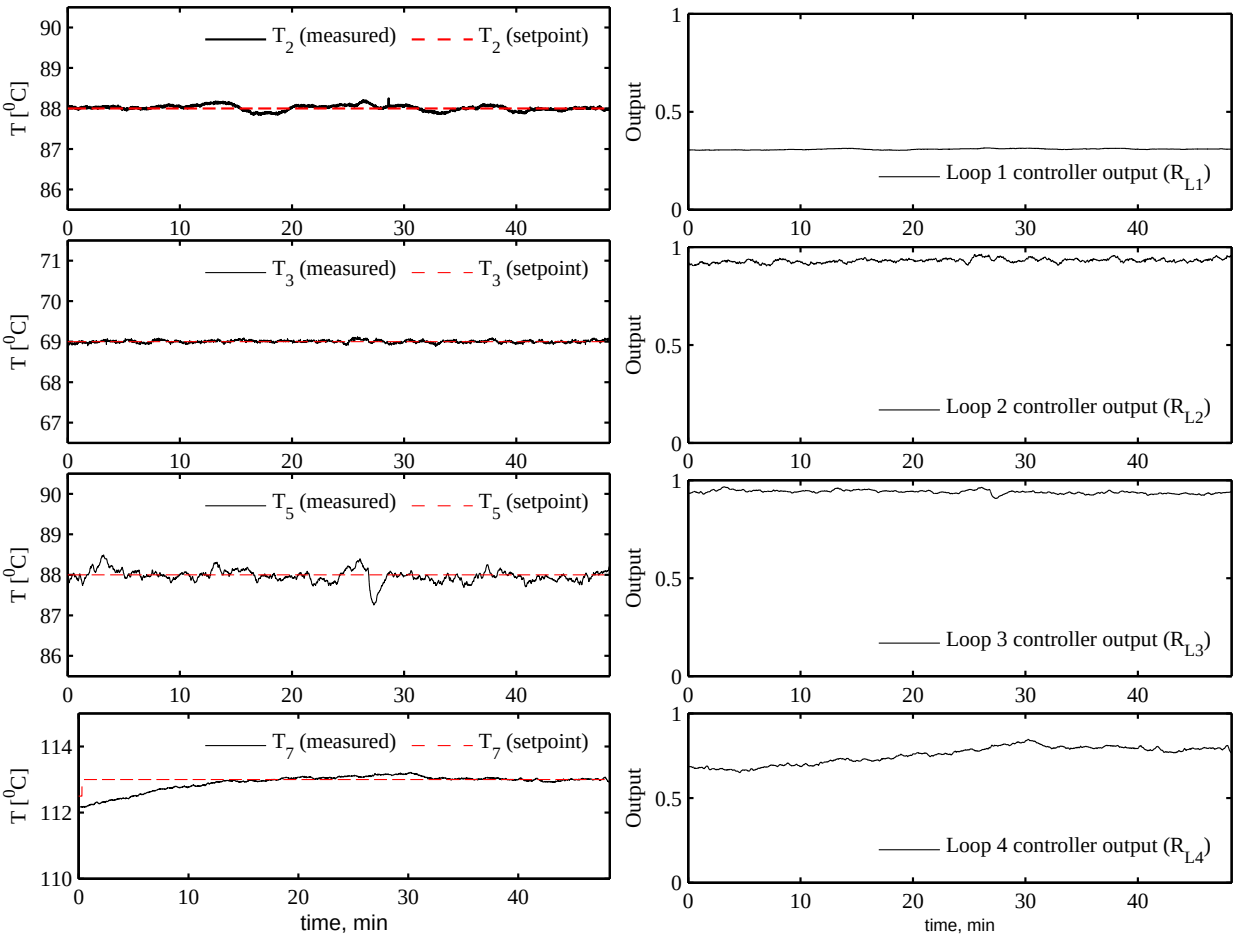

Figure 13: Experimental Run 9: steady state operation ($T_{2S} = 88^0$C $T_{3S} = 69^0$C $T_{5S} = 88^0$C $T_{7S} = 113^0$C)

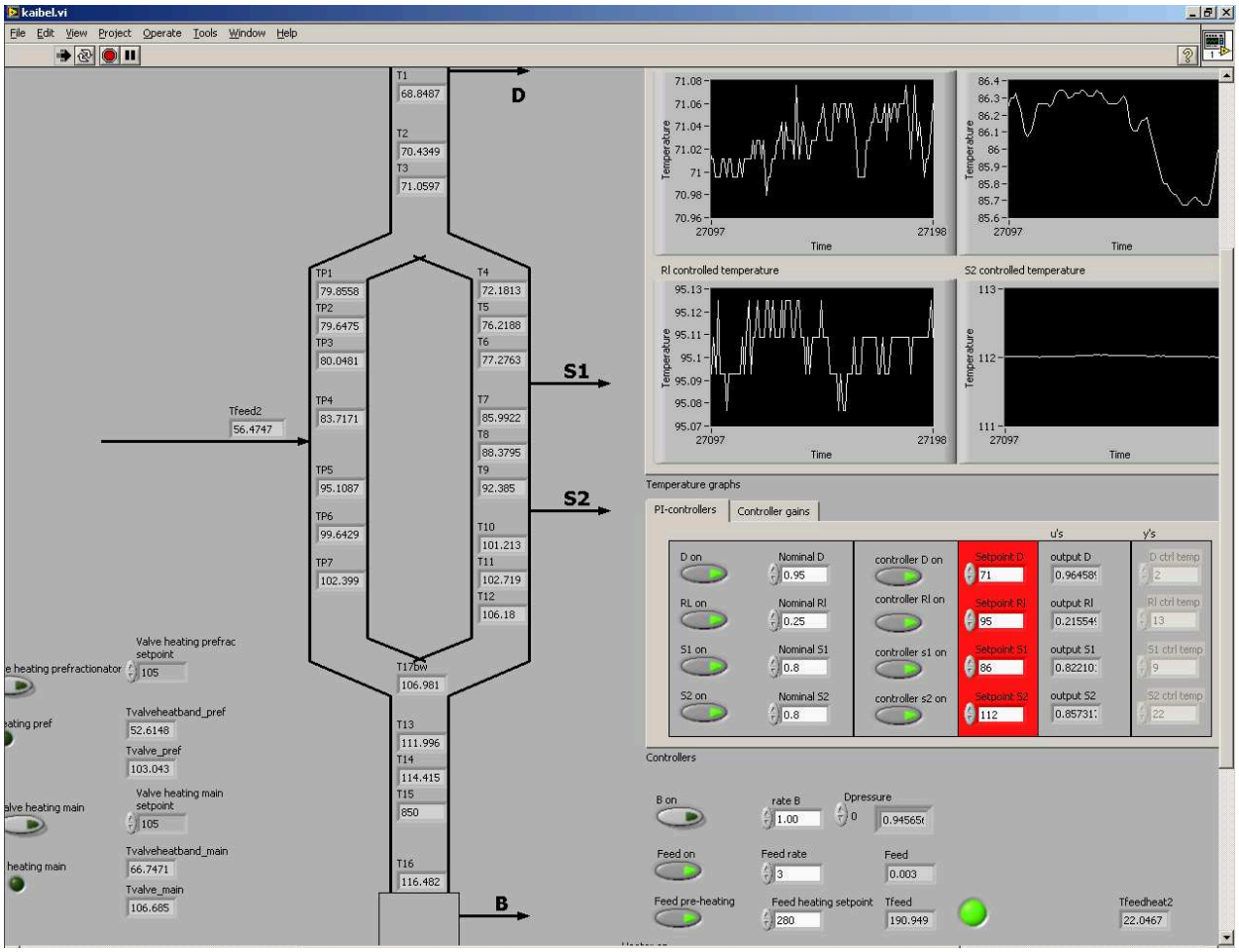

Figure 14: Screenshot of operator interface during experimental run 12

liquid phase and the vapor is assumed to be ideal. We use the constant molar overflow assumption, which is reasonable for our mixture.

To match the experimental steady state data, we can adjust the following degrees of freedom in the model:

1. number of theoretical stages (we use a fixed value for all experiments)
2. boilup (V/F)
3. feed composition
4. liquid split ratio (R_{L1})
5. vapor split ratio (R_V)
6. distillate product split ratio (R_{L2})
7. upper side product split ratio (R_{L3})
8. lower side product split ratio (R_{L4})

The degrees of freedom are adjusted for each experiment, except for the number of theoretical number of stages in the sections. The number of theoretical stages was based on experimental estimation of the height equivalent of a theoretical plate (HETP). For this, a total reflux experiment (run 13) was performed with only two components, namely methanol and ethanol. The liquid split ratio (R_{L1}) was used to control temperature difference ($\Delta T = T_2 - T_5$) between the prefractionator (section 2) and in the main column (section 5). The temperatures ($T_2 \equiv TP5, T_5 \equiv TM8$) chosen were approximately at the same height (and of packing) from the reboiler. The setpoint of this controller was then set to *zero* so that the compositions should be same on both sides. The system was allowed to stabilize and samples were taken at the location of side products (S1 and S2) for analysis. Figure 15 shows the stable run during this experiment with the controlled-variable (ΔT) and controller output. The height of packing between the sample points is 0.65 meters. The molar composition of methanol was about 75 % and 21 % in samples S1 and S2, respectively, and from

this the total number of theoretical stages in the section between the side streams was estimated to be about 4. The HETP was thus found to be about 16 *cm*. By assuming the same HETP in the rest of the column we determine the number of theoretical stages in each section. Based on this, the number of theoretical stages used in the simulations is 13 in the prefractionator (5+8) and 22 in the main column (4+4+4+4+4+5+reboiler).

Based on the power input of 2 kW to the reboiler, we estimate the boilup (V/F) for use in the model. The feed composition is available from HPLC measurements. Finally, the experimental liquid split ratio (R_{L1}) can be obtained directly from the experiments.

With the first *four* degree of freedom determined, we are left with *four* more degrees of freedom, which are determined as follows.

The distillate product split ratio (R_{L2}) in the model is adjusted to match the measured mole fraction of methanol in the top product (D). The upper side product split ratio (R_{L3}) in the model is adjusted to match the measured mole fraction of ethanol in the upper side product (S1). The lower side product split ratio (R_{L4}) in the model is adjusted to match the measured mole fraction of propanol in lower side product (S2). Finally, the vapor split ratio in the model (R_V) is adjusted to match a temperature in section 2 (TP5) of the prefractionator.

The same procedure is used for experiment runs 9-12 and Table 3 compares the product composition from experiments and simulations. Since the mole fractions of the main components in the top product (D), upper side product (S1) and lower side product (S2) are matched directly, there is an exact match of these compositions. But additionally, the key impurities in the side products (S1 & S2), which were not matched individually, show a very good fit. For example, in experimental run 9, the mole fraction of methanol in S1 from experiments is 31.8%, while from the simulations it is 32.0%. The key impurities (propanol and n–butanol) of the lower side product (S2) also show a good fit.

Figure 16 compares the temperatures from the model (lines) and the experiments (points). The *y-axis* in Figure 16 shows the theoretical stages in the model, numbered from top (1) to bottom (22). The *x-axis* shows the corresponding temperatures. The locations of temperature probes in

experimental setup with respect to the theoretical stages in the model are not precise and were not adjusted, but nevertheless we find that the match is good.

In summary, we have a very good agreement between the experimental steady-state data and the equilibrium stage model.

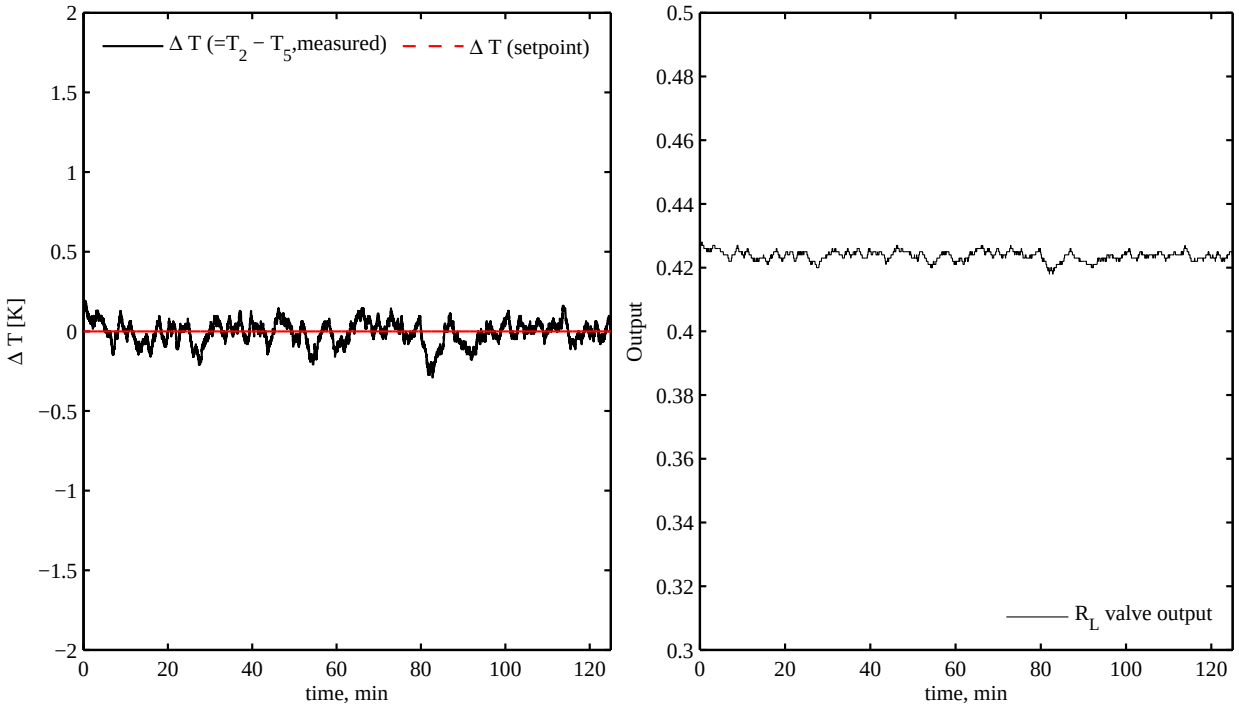

Figure 15: Experimental Run 13: total reflux conditions for determining the HETP and for estimating the experimental vapor split

Discussion

Practical issues related to operation

The operation of the experimental column had some problems. Early on, the column was very difficult to operate and stabilize with little material reaching the top of the column.[20] Unlike the intuition that suggests that this was due to insufficient boilup, the reason turned out to be vapor leaking from the product valves on the side streams. To resolve this issue, we installed an additional small manual valve and a solenoid valve (in series) downstream the swinging funnels, just outside

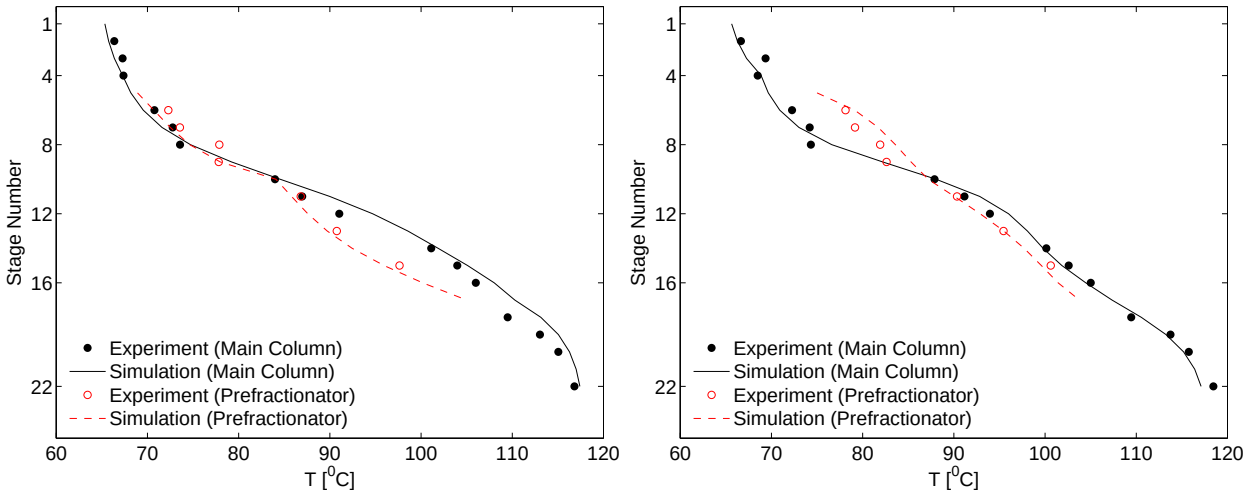

(a) Experiment Run 9

(b) Experiment Run 10

(c) Experiment Run 11

(d) Experiment Run 12

Figure 16: Steady state experimental and simulated temperature profiles in experiments 9-12

the column. The opening of the manual valve was adjusted to ensure that there was always a liquid hold up in the glass downcomer under the swinging funnel. The additional solenoid valves and the swinging funnel open and close simultaneously during the cycle. Alternatively, an externally placed liquid seal in the product withdrawal line would have stopped any vapor from "leaking" by providing a hydraulic head to counter the small positive pressure in the column.

Plant-model mismatch

As mentioned, the equilibrium stage model fits well with the experiments. The mole fraction of butanol in the bottoms product was, however, smaller than that in the model in all the runs. One reason for this may be, that we have no bottom product (B), meaning that the bottom product accumulates in the reboiler, and therefore it will take a very long time to reach the steady compositions in the reboiler.

The experimental data also had some uncertainties. The experimental results as shown in Figure 12 also show some noise in the temperatures. This can be just instrument noise or process noise due to the use of swinging funnels and not continuous valves with pumps. The composition measurements with HPLC also have some measurement error. There were some biases in temperature probes. These were calibrated using their measurements in cold column conditions. Some probes showed up to 3 ^{0}C of error from the room temperature and their measurements were accordingly corrected.

Another source of error can be the column pressure drop, which was neglected in the model. The total pressure drop under normal operation of the column was about 16 *cm* of water or about 0.016 bar (measured using a U-tube manometer).

Experimental vapor split

The total-reflux experiment provides information about the actual vapor split ratio, which is set by the natural pressure drop as offered by the packing. Due to the mass balance requirements, the vapor split ratio (R_V) under the total reflux conditions with the same temperature on both

sides ($\Delta T = 0$ K), must be equal to experimental liquid split ratio (R_L) which is equal to about 0.42 (Figure 15). However, in the other experiments, when the feed is introduced, one would expect lesser vapor to go to the prefractionator (so R_V is smaller) because the additional liquid flow provides more resistance and this is what we observe indeed, from the simulation results in Table 4, we find that R_V is between 0.31 and 0.39 in the four experimental runs.

Optimal operation

From the experimental data and the model in table 3, the purities of top and bottom products are relatively high (up to about 96% and 95 %), while the purities of the side products are low (about 55% and 89 %). Is this the best one can achieve? We can use the model to the compare the four experimental steady-state runs to an optimized operation.

We consider two practical modes of operation. In mode I, for the given boilup, the purity of top product (x^D_{MeOH}) and bottom product (x^B_{BuOH}) is specified and the objective is to maximize the sum of the purities of the side products ($J = x^{S1}_{EtOH} + x^{S2}_{PrOH}$). In mode II, we define as our objective to maximize the sum of purities of all the products ($J = x^D_{MeOH} + x^{S1}_{EtOH} + x^{S2}_{PrOH} + x^B_{BuOH}$).

The two optimization problems, named as mode I and mode II are defined in table 5 and the results are given in Table 6.

In mode I, where the top and bottom purities are fixed, we find that little improvement can be made in the purities. In experimental run 11, the S1 purity can be improved from 51.5 % to 65.3 %. The purity of side stream 2, however, is smaller in all the four runs.

In mode II, even though there was an improvement on the sum of the purities of four products, the purity of the end products (D and B) decreased from the base case and the purity of the upper side products (S1) increased in all the scenarios while the purity if lower side product decreased in experimental runs 10-12. From the purity figures in table 6, we can conclude that the experimental results are close to the “optimal” operations, as described by mode I or mode II. This shows that the temperature setpoint adjustments mentioned in the start-up procedure works well.

Conclusions

The experimental studies verify that stable operation of the four product Kaibel column can be achieved with the 4-point temperature control scheme shown in figure 3c. The control structure gave good servo performance for several setpoint changes and gave good regulation for a +20 % feed disturbance. The same control structure was adopted during the cold start-up of the column and with the proposed procedure for adjusting the temperature setpoints, it was possible to use only temperature measurements to approach the desired steady-state composition that is, without needing online composition measurements.

An equilibrium stage model was fitted to the experiments. The fitted model gave good match with the experiments. This suggests that such staged models can be used to study the operation and design of larger industrial scale Kaibel columns.

Acknowledgement

Ms. Kathinka Qvenild Lystad, Engineer, SINTEF Materials and Chemistry, assisted with the HPLC analysis of samples.

References

1. Petlyuk, F.; Platonov, V.; Avetlyan, V. Optimum Arrangements in the Fractionating Distillation of Multicomponent Mixtures. *Khimicheskaya Promyshlennost* **1966**, *42*, 865–868.

2. Kaibel, G. Distillation columns with vertical partitions. *Chemical Engineering & Technology* **1987**, *10*, 92–98.

3. Fonyó, Z. Thermodynamic analysis of rectification. I. Reversible Model of rectification. *International Chemical Engineering* **1974**, *14*, 18–26.

4. Fonyó, Z. Thermodynamic analysis of rectification. II. Finite cascade models. *International Chemical Engineering* **1974**, *14*, 203–210.

5. Petlyuk, F.; Platonov, V.; Slavinskii, D. Thermodynamically optimal method for separating multicomponent mixtures. *International Chemical Engineering* **1965**, *5*, 555–561.

6. Petlyuk, F.; Platonov, V. Thermodynamically reversible multicomponent distillation. *Khimicheskaya Promyshlennost* **1964**, 723–726 (In Russian).

7. Kaibel, G. 1984; A distillation column for fractionating multicomponent feed (German Title: Destillationskolonne zur destillativen Zerlegung eines aus mehreren Fraktionen bestehenden Zulaufproduktes), European Patent EP 0 122 367 A2, 1984 (1984); Priority data DE 3302525 (1983).

8. Halvorsen, I. J.; Skogestad, S. Minimum Energy Consumption in Multicomponent Distillation. 3. More Than Three Products and Generalized Petlyuk Arrangements. *Industrial & Engineering Chemistry Research* **2003**, *42*, 616–629.

9. Olujic, Z.; Jödecke, M.; Shilkin, A.; Schuch, G.; Kaibel, B. Equipment improvement trends in distillation. *Chemical Engineering and Processing: Process Intensification* **2009**, *48*, 1089–1104.

10. Dividing wall column, A breakthrough towards sustainable distilling. *Chemical Engineering and Processing: Process Intensification* **2010**, *49*, 559 – 580.

11. Niggemann, G.; Hiller, C.; Fieg, G. Experimental and Theoretical Studies of a Dividing-Wall Column Used for the Recovery of High-Purity Products. *Industrial & Engineering Chemistry Research* **2010**, *49*, 6566–6577.

12. Niggemann, G.; Gruetzmann, S.; Fieg, G. Distillation startup of fully thermally coupled distillation columns: theoritical examination. 2006.

13. Mutalib, M. I. A.; Smith, R. Operation and Control of Dividing Wall Distillation Columns: Part 1: Degrees of Freedom and Dynamic Simulation. *Chemical Engineering Research and Design* **1998**, *76*, 308–318.

14. Mutalib, M. I. A.; Zeglam, A. O.; Smith, R. Operation and Control of Dividing Wall Distillation Columns: Part 2: Simulation and Pilot Plant Studies Using Temperature Control. *Chemical Engineering Research and Design* **1998**, *76*, 319–334.

15. Adrian, T.; Schoenmakers, H.; Boll, M. Model predictive control of integrated unit operations: Control of a divided wall column. *Chemical Engineering and Processing* **2004**, *43*, 347–355.

16. Ling, H.; Luyben, W. L. New Control Structure for Divided-Wall Columns. *Industrial & Engineering Chemistry Research* **2009**, *48*, 6034–6049.

17. Strandberg, J.; Skogestad, S. *Proceedings of IFAC International Symposium on Advanced Control of Chemical Processes (ADCHEM 2006), Gramado, Brazil*; 2006; Vol. 2; pp 623–628.

18. Ghadrdan, M.; Halvorsen, I. J.; Skogestad, S. Optimal operation of Kaibel distillation columns. *Chemical Engineering Research and Design* **2011**, *89*, 1382 – 1391, Special Issue on Distillation & Absorption.

19. Kvernland, M.; Halvorsen, I. J.; Skogestad, S. Model Predictive Control of a Kaibel Distillation Column. 2010.

20. Strandberg, J. Optimal operation of dividing wall columns. Ph.D. thesis, Norwegian University of Science and Technology, Department of Chemical Engineering,Trondheim, Norway, 2011.

21. Skogestad, S. Simple analytic rules for model reduction and PID controller tuning. *Journal of Process Control* **2003**, *13*, 291–309.

Table 2: List of experiments [a]

Experiment	Description
Run 1	cold start-up
Run 2	$-2\ [^0C]$ setpoint change in T_2 (prefractionator loop)
Run 3	$\pm 1\ [^0C]$ setpoint changes in T_3 (distillate product loop)
Run 4	$\pm 1\ [^0C]$ setpoint changes in T_5 (upper side product loop)
Run 5	$\pm 1\ [^0C]$ setpoint changes in T_7 (lower side product loop)
Run 6	simultaneous $\pm 1\ [^0C]$ setpoints changes in all temperatures
Run 7	+20 % disturbance in feed rate
Run 8	steady state run with constant setpoints: $T_2 = 80.6\ ^0C\ T_3 = 69\ ^0C\ T_5 = 82\ ^0C\ T_7 = 110.2\ ^0C$
Run 9	steady state run with constant setpoints: $T_2 = 88^0C\ T_3 = 69^0C\ T_5 = 88^0C\ T_7 = 113^0C$
Run 10	steady state run with constant setpoints: $T_2 = 91^0C\ T_3 = 69.5^0C\ T_5 = 92^0C\ T_7 = 113^0C$
Run 11	steady state run with constant setpoints: $T_2 = 91.5^0C\ T_3 = 72^0C\ T_5 = 92^0C\ T_7 = 112^0C$
Run 12	steady state run with constant setpoints: $T_2 = 95^0C\ T_3 = 71^0C\ T_5 = 86^0C\ T_7 = 112^0C$
Run 13	total reflux experiment for calculating number of theoretical stages

[a] Feed rate for all runs (except run 7) = 3 LPH
Reboiler duty for all runs = 2 kW

Table 3: Steady state experimental and simulated compositions in runs 9-12

Experiment Run 9									
	Feed	D		S1		S2		B	
Component	exp & sim	exp	sim	exp	sim	exp	sim	exp	sim
methanol (mol %)	**21.4**	**96.6**	**96.6**	31.8	32.0	0	1.04	0	0
ethanol (mol %)	**15.4**	3.4	3.4	**55.4**	**55.4**	16.8	13.7	0	0
propanol (mol %)	**21.4**	0	0	12.7	12.4	**75.0**	**75.0**	7.4	1.6
n-butanol (mol %)	**41.7**	0	0	0	0	8.2	10.1	92.6	98.4
Experiment Run 10									
	Feed	D		S1		S2		B	
Component	exp & sim	exp	sim	exp	sim	exp	sim	exp	sim
methanol (mol %)	**20.4**	**94.9**	**94.9**	29.9	27.42	0	0.6	0	0
ethanol (mol %)	**27.4**	5.1	5.1	**51.2**	**51.2**	5.9	7.2	0	0
propanol (mol %)	**28.5**	0	0	18.9	21.3	**87.5**	**87.5**	4.6	2.6
n-butanol (mol %)	**23.7**	0	0	0	0	6.6	4.6	95.4	97.3
Experiment Run 11									
	Feed	D		S1		S2		B	
Component	exp & sim	exp	sim	exp	sim	exp	sim	exp	sim
methanol (mol %)	**20.4**	**92.7**	**92.7**	17.3	15.0	0	0.2	0	0
ethanol (mol %)	**17.6**	7.3	7.3	**51.5**	**51.5**	5.4	4.6	0	0
propanol (mol %)	**26.7**	0	0	31.2	33.3	**89.6**	**89.6**	6.7	3.1
n-butanol (mol %)	**35.3**	0	0	0	0	4.9	5.5	93.3	96.9
Experiment Run 12									
	Feed	D		S1		S2		B	
Component	exp & sim	exp	sim	exp	sim	exp	sim	exp	sim
methanol (mol %)	**16.3**	**94.4**	**94.4**	26.3	22.63	0	0.5	0	0
ethanol (mol %)	**19.0**	5.6	5.6	**56.3**	**56.3**	10.1	8.5	0	0
propanol (mol %)	**28.3**	0	0	17.3	20.9	**86.3**	**86.3**	6.4	3.3
n-butanol (mol %)	**36.4**	0	0	0	0	3.5	4.7	93.6	96.7

Table 4: Inputs in the four experiments 9-12

	Experiment Run 9		Experiment Run 10		Experiment Run 11		Experiment Run 12	
Input	exp	sim	exp	sim	exp	sim	exp	sim
R_{L1}	**0.31**	**0.31**	**0.15**	**0.15**	**0.25**	**0.25**	**0.21**	**0.21**
R_{L2}	0.93	0.95	0.98	0.97	0.93	0.95	0.96	0.97
R_{L3}	0.94	0.90	0.72	0.81	0.81	0.87	0.83	0.88
R_{L4}	0.75	0.87	0.83	0.91	0.90	0.91	0.86	0.88
R_V	-	0.39	-	0.31	-	0.35	-	0.33

Table 5: Operation under two optimal modes

	Mode I	Mode II
Objective	$J = x^{S1}_{EtOH} + x^{S2}_{PrOH}$	$J = x^{D}_{MeOH} + x^{S1}_{EtOH} + x^{S2}_{PrOH} + x^{B}_{BuOH}$
Constraints	Feed Rate = nominal Feed Composition = nominal Feed Composition = nominal Feed liquid fraction = Nominal boilup = nominal x^{D}_{MeOH} = nominal x^{B}_{BuOH} = nominal	Feed Rate = nominal Feed Composition = nominal Feed Composition = nominal Feed liquid fraction = Nominal boilup = nominal

Table 6: Comparison of experiments 9-12 with optimal operation in mode I (maximize sum of the purities of side products) and mode II (maximize sum of the purities of all the products).

Experiment Run 9												
	D			S1			S2			B		
	nom	mode		nom	mode		nom	mode		nom	mode	
component		I	II		I	II		I	II		I	II
Methanol	96.6	96.6	89.6	32.1	24.9	12.2	1.0	0.8	0.4	0.0	0.0	0.0
Ethanol	3.4	3.4	10.4	55.4	59.9	70.2	13.7	15.7	13.0	0.0	0.0	0.0
Propanol	0.0	0.0	0.0	12.4	15.2	17.6	75.0	73.4	83.1	1.6	1.5	4.1
Butanol	0.0	0.0	0.0	0.1	0.1	0.0	10.2	10.1	3.6	98.4	98.4	95.9
Experiment Run 10												
	D			S1			S2			B		
	nom	mode		nom	mode		nom	mode		nom	mode	
component		I	II		I	II		I	II		I	II
Methanol	94.9	94.9	88.9	27.4	27.0	13.6	0.6	0.7	0.4	0.0	0.0	0.0
Ethanol	5.1	5.1	11.1	51.2	54.6	69.9	7.3	9.3	12.9	0.0	0.0	0.0
Propanol	0.0	0.0	0.0	21.3	18.3	16.4	87.5	85.4	83.0	2.6	2.6	3.3
Butanol	0.0	0.0	0.0	0.1	0.1	0.0	4.6	4.7	3.7	97.4	97.4	96.7
Experiment Run 11												
	D			S1			S2			B		
	nom	mode		nom	mode		nom	mode		nom	mode	
component		I	II		I	II		I	II		I	II
Methanol	92.7	92.7	89.4	15.0	17.8	13.0	0.2	0.5	0.4	0.0	0.0	0.0
Ethanol	7.3	7.3	10.6	51.5	65.3	71.0	4.7	12.0	13.4	0.0	0.0	0.0
Propanol	0.0	0.0	0.0	33.4	16.8	16.0	89.6	82.9	82.2	3.1	3.1	3.5
Butanol	0.0	0.0	0.0	0.1	0.0	0.0	5.5	4.6	4.0	96.9	96.9	96.5
Experiment Run 12												
	D			S1			S2			B		
	nom	mode		nom	mode		nom	mode		nom	mode	
component		I	II		I	II		I	II		I	II
Methanol	94.4	94.4	94.5	22.6	23.4	23.5	0.6	0.6	0.6	0.0	0.0	0.0
Ethanol	5.6	5.6	5.5	56.3	57.8	57.9	8.4	9.1	9.4	0.0	0.0	0.0
Propanol	0.0	0.0	0.0	21.0	18.8	18.5	86.3	85.4	86.0	3.1	3.1	3.8
Butanol	0.0	0.0	0.0	0.1	0.1	0.0	4.7	4.9	3.9	96.9	96.9	96.2